Survey of $E1$ transitions in the mass $A\sim 60$ region

O. Izotova,[1] D. Rudolph,[1] J. Ekman,[1] C. Fahlander,[1] A. Algora,[2,*] C. Andreoiu,[1,†] R. Cardona,[3] C. Chandler,[4,‡] G. de Angelis,[2] E. Farnea,[2,§] A. Gadea,[2] J. Garcés Narro,[4] J. Nyberg,[5] M. Palacz,[6] Zs. Podolyák,[4] T. Steinhardt,[7] and O. Thelen[7]

[1]*Department of Physics, Lund University, S-22100 Lund, Sweden*
[2]*Laboratori Nazionali di Legnaro, I-35020 Legnaro, Italy*
[3]*Departmento de Física, Universidad Nacional de Colombia, Bogotá, Colombia*
[4]*Department of Physics, University of Surrey, Guildford, GU 2 7XH, United Kingdom*
[5]*The Svedberg Laboratoriet, S-75121 Uppsala, Sweden*
[6]*Heavy Ion Laboratory, University of Warsaw, PL-02-093 Warsaw, Poland*
[7]*Institut für Kernphysik, Universität zu Köln, D-50937 Köln, Germany*

(Received 26 January 2004; published 25 March 2004)

A survey of parity-changing $E1$ transitions has been pursued in $N\gtrsim Z$ nuclei near ^{56}Ni using data from an EUROBALL experiment. Linear polarization measurements have been combined with angular correlations of coincident γ rays to determine the electromagnetic character of numerous transitions. The impact of the results on shell-model parametrizations is briefly discussed.

DOI: 10.1103/PhysRevC.69.037303 PACS number(s): 27.50.+e, 21.60.Cs, 23.20.En, 23.20.Lv

Doubly magic nuclei and their nearby neighbors are of specific interest in nuclear structure studies because they are the prominent testing ground for the spherical shell model and its parametrizations. Recent high-spin γ-ray spectroscopic studies of nuclei just above ^{56}Ni, e.g., Refs. [1–4], have shown that despite the fact that they are lying in the heart of the fp shell the $l=4$, $1g_{9/2}$ intruder orbital is important for the understanding of moderately excited levels or sometimes even low-spin states in these nuclei. This manifests in difficulties of modern large-scale shell-model theory in describing these nuclei, because a proper model space and interaction comprising both the fp shell and the $1g_{9/2}$ orbital cannot readily be derived [5]. Important experimental input concerning this problem is the unambiguous identification of parity changing transitions, as each change in parity is associated with the excitation of a particle from the fp shell into the $1g_{9/2}$ orbital. The present experimental study aims at such key transitions by a survey of angular correlation and linear polarization measurements in neutron-deficient mass $A\sim 60$ nuclei.

The experiment was performed at the Laboratori Nazionali di Legnaro in Italy using a 96 MeV ^{24}Mg beam, which was provided by the Tandem XTU accelerator, and a 0.5 mg/cm^2 thin ^{40}Ca target. The ^{40}Ca layer was backed by 7 mg/cm^2 gold and on the front it was protected against oxidation with a flash of gold. The γ radiation following the fusion-evaporation reaction was detected in the EUROBALL Ge-detector array [6] consisting of 26 CLOVER detectors [7] (13 at 77° and 13 at 103° relative to the beam axis) and 15 CLUSTER detectors [8] (5 at 103°, 5 at 135°, and 5 at 156°). The 1π forward section of EUROBALL was covered with the 50 liquid scintillator elements of the EUROBALL Neutron Wall [9] to measure evaporated neutrons, while evaporated charged particles were detected in the 40-element silicon ΔE-E array ISIS [10].

Directional correlations between oriented states (DCO) have been investigated with γ rays detected in the CLUSTER ring at $\Theta=156°$ and the CLOVER section ($\Theta=77°$ and $\Theta=103°$) by means of DCO ratios [11]

$$R_{DCO}=\frac{I(\gamma_1 \text{ at } 156°;\ \text{gated with } \gamma_2 \text{ at } 77°,103°)}{I(\gamma_1 \text{ at } 77°,103°;\ \text{gated with } \gamma_2 \text{ at } 156°)}. \quad (1)$$

Note that the CLOVER detectors at 77° and 103° are equivalent as far as DCO ratios are concerned. The numbers presented in Table I involve a correction for detection efficiencies, which has been applied to both the gated and projected γ rays. Line shapes from Doppler shift attenuation effects may occur for transitions from short-lived states due to γ-ray emission during the slowing down process of the recoils in the gold backing. If the lifetime is not too short, i.e., if a major fraction of the line shape comes from γ-ray emission from stopped recoils, the effect can easily be accounted for by performing an integration to determine the full yield of a transition in a spectrum, instead of the conventional least-squares fit to a sharp Gaussian peak shape. Known stretched $E2$ transitions were used for gating, such that $R_{DCO}=1.0$ is expected for stretched quadrupole transitions and $R_{DCO}\sim 0.6$ for stretched dipoles, while nonstretched $\Delta I=0$ transitions have values similar to stretched quadrupole transitions.

The linear polarization and, consequently, the electric or magnetic character of the radiation can typically (see, e.g., Ref. [12]) be determined through a normalized difference between the number of Compton scattered γ rays in the reaction plane $N_{\|}$, and perpendicular to it, $N_{\perp}$. They are measured in either dedicated Compton polarimeters (see, e.g.,

*Present address: Institute of Nuclear Research, H-4001 Debrecen, Hungary.
†Present address: Department of Physics, University of Guelph, Guelph, Ontario, Canada N1G 2W1.
‡Present address: School of Chemistry and Physics, Keele University, Keele, Staffordshire, ST5 5BG, UK.
§Present address: Dipartmento di Fisica dell'Universitá and INFN, Sezione di Padova, I-35141 Padova, Italy.

TABLE I. Excitation and transition energies in keV and their measured angular correlations R_{DCO} and anisotropies A along with the assigned multipole character $T\lambda$ and deduced spins of initial and final states in ^{61}Zn, ^{60,61}Cu, $^{57-60}$Ni, and ^{57}Co.

E_x	E_γ	R_{DCO}	A	$T\lambda$	I_i	I_f
	^{61}Zn+2p1n					
124	124	0.38(3)		$E2/M1$	$5/2^-$	$3/2^-$
996	873	0.30(4)	+0.041(12)	$E2/M1$	$7/2^-$	$5/2^-$
	996[a]	0.99(6)	+0.071(62)	$E2$	$7/2^-$	$3/2^-$
1265	1141	1.15(9)	+0.096(25)	$E2$	$9/2^-$	$5/2^-$
2270	1273		+0.096(38)	$E2$	$11/2^-$	$7/2^-$
2399	1403	0.54(4)	+0.063(13)	$E1$	$9/2^+$	$7/2^-$
2797	1532	0.91(7)	+0.027(75)	$E2$	$13/2^-$	$9/2^-$
3336	937	1.11(7)	+0.087(12)	$E2$	$13/2^+$	$9/2^+$
	1066	0.45(6)	+0.138(52)	$E1$	$13/2^+$	$11/2^-$
4264	1467	0.44(4)	+0.074(31)	$E1$	$15/2^+$	$13/2^-$
4415	1079	0.99(6)	+0.072(14)	$E2$	$17/2^+$	$13/2^+$
4645	1849	1.00(12)	+0.122(54)	$E2$	$17/2^-$	$13/2^-$
5553	1289	0.88(7)	+0.103(30)	$E2$	$19/2^+$	$15/2^+$
6090	1675[a]	0.91(6)	+0.059(20)	$E2$	$21/2^+$	$17/2^+$
7486	1396	0.94(7)	+0.094(69)	$E2$	$25/2^+$	$21/2^+$
7629	1538	0.48(3)	+0.090(17)	$E1$	$23/2^-$	$21/2^+$
9162	1534	0.95(7)	+0.039(22)	$E2$	$27/2^-$	$23/2^-$
10156	994[a]	0.99(6)	+0.125(36)	$E2$	$31/2^-$	$27/2^-$
	^{61}Cu+3p					
970	970	0.30(2)	+0.015(13)	$E2/M1$	$5/2^-$	$3/2^-$
1310	340	0.56(4)	−0.104(23)	$M1$	$7/2^-$	$5/2^-$
	1310	1.04(4)	+0.104(9)	$E2$	$7/2^-$	$3/2^-$
1733	422	1.28(6)	+0.105(15)	$\Delta I=0$	$7/2^-$	$7/2^-$
	1733	1.04(4)	+0.062(20)	$E2$	$7/2^-$	$3/2^-$
1942	972		−0.044(24)	$M1$	$7/2^-$	$5/2^-$
2336	1026	0.40(5)	+0.031(33)	$E2/M1$	$9/2^-$	$7/2^-$
	1366		+0.110(18)	$E2$	$9/2^-$	$5/2^-$
2627	1316	1.04(4)	+0.082(16)	$E2$	$11/2^-$	$7/2^-$
2721	988	0.52(3)	+0.050(17)	$E1$	$9/2^+$	$7/2^-$
	1410	0.51(3)	+0.064(10)	$E1$	$9/2^+$	$7/2^-$
3016	1705[a]	0.90(4)	+0.055(22)	$E2$	$11/2^-$	$7/2^-$
3260	1527	1.02(9)	+0.108(48)	$E2$	$11/2^-$	$7/2^-$
3780	1444	1.07(9)	+0.050(37)	$E2$	$13/2^-$	$9/2^-$
4082	1065	0.52(3)	+0.028(14)	$E1$	$13/2^+$	$11/2^-$
	1361	1.02(4)	+0.115(15)	$E2$	$13/2^+$	$9/2^+$
4591	1330	0.69(5)	+0.069(21)	$E1$	$13/2^+$	$11/2^-$
	1870	1.12(6)	+0.108(27)	$E2$	$13/2^+$	$9/2^+$
5120	529	1.04(5)	+0.101(11)	$E2$	$17/2^+$	$13/2^+$
	1038	0.95(4)	+0.063(16)	$E2$	$17/2^+$	$13/2^+$
5856	736	0.65(8)	−0.137(17)	$M1$	$19/2^+$	$17/2^+$
6824	1704[a]	0.90(4)	+0.075(22)	$E2$	$21/2^+$	$17/2^+$
7389	564[a]	0.57(6)		$M1$	$23/2^+$	$21/2^+$
	1532	1.02(10)	+0.060(19)	$E2$	$23/2^+$	$19/2^+$
7937	1112	0.51(2)	+0.056(14)	$E1$	$23/2^-$	$21/2^+$
9408	1472	1.12(8)	+0.113(17)	$E2$	$27/2^-$	$23/2^-$
	^{60}Cu+3p1n					
287	225	0.52(9)	−0.097(27)	$M1$	2^+	1^+
	287[a]		+0.051(33)	$\Delta I=0$	2^+	2^+
454	454	0.44(3)	−0.061(7)	$E2/M1$	3^+	2^+
558	270	0.90(11)	+0.125(22)	$E2$	4^+	2^+
	558	1.05(7)	+0.084(6)	$E2$	4^+	2^+
1604	1046	0.25(2)	+0.006(5)	$E2/M1$	5^+	4^+
1779	1221	0.67(7)	+0.022(30)	$E2/M1$	5^+	4^+
	1325		+0.073(30)	$E2$	5^+	3^+
2027	1469	0.68(9)	−0.011(13)	$E2/M1$	5^+	4^+
	1573		+0.090(45)	$E2$	5^+	3^+
2197	1640	0.94(6)	+0.060(6)	$E2$	6^+	4^+
2692	1088	0.29(6)	+0.002(17)	$E2/M1$	6^+	5^+
2817	790	0.85(15)	−0.079(49)	$E2/M1$	6^+	5^+
3156	1129[a]		+0.065(11)	$E1$	6^-	5^+
	1552	0.56(3)	+0.029(10)	$E1$	6^-	5^+
3191	1587	0.95(14)	+0.071(17)	$E2$	7^+	5^+
3354	1157	0.49(3)	+0.051(5)	$E1$	7^-	6^+
4521	1166	0.23(5)	+0.026(18)	$E2/M1$	8^-	7^-
	1330	0.46(8)	+0.039(19)	$E1$	8^-	7^+
	1365	0.96(13)	+0.086(15)	$E2$	8^-	6^-
5188	1416	1.03(12)	+0.060(19)	$E2$	9^-	7^-
	1833	1.15(17)	+0.054(16)	$E2$	9^-	7^-
5648	461	0.50(6)	−0.084(11)	$M1$	10^-	9^-
	1128[a]	1.00(5)	+0.070(9)	$E2$	10^-	8^-
6094	446	0.38(8)	−0.019(19)	$E2/M1$	11^-	10^-
	906	0.90(11)	+0.075(18)	$E2$	11^-	9^-
7394	1746	0.51(4)	+0.046(8)	$E1$	11^+	10^-
8132	738	1.05(6)	+0.099(6)	$E2$	13^+	11^+
	2038	1.19(32)	−0.136(46)	$M2$	13^+	11^-
	^{60}Ni+4p					
5014	1894	0.41(3)	+0.047(36)	$E1$	5^-	4^+
	2507	0.46(5)	+0.053(27)	$E1$	5^-	4^+
5348	334	0.93(4)	+0.113(17)	$E2$	7^-	5^-
	363	0.51(3)	+0.092(19)	$E1$	7^-	6^+
	1083	0.48(2)	+0.046(4)	$E1$	7^-	6^+
	2842	1.31(17)	+0.122(74)	$E3$	7^-	4^+
	^{59}Ni+4p ln					
3054	1106	0.52(3)	+0.028(30)	$E1$	$9/2^+$	$7/2^-$
	1717	0.57(5)	+0.045(26)	$E1$	$9/2^+$	$7/2^-$
4454	1750	0.48(3)	+0.013(15)	$E1$	$13/2^+$	$11/2^-$
	^{58}Ni+1α2p					
6083	700	0.46(4)	+0.039(19)	$E1$	7^-	6^+
	956	0.59(3)	+0.054(15)	$E1$	7^-	6^+
7273	2146	0.48(15)	+0.048(30)	$E1$	7^-	6^+
	^{57}Ni +1α2p1n					
3701	1124	0.57(5)	+0.029(22)	$E1$	$9/2^+$	$7/2^-$
	^{57}Co+1α3p					
4845	3155	0.56(4)	+0.032(10)	$E1$	$13/2^+$	$11/2^-$

[a]Doublet structure.

Ref. [13]) or composite detectors such as the EUROBALL CLOVER detectors [7], which have to be positioned near 90° relative to the beam axis, where the polarization is largest [12]. This is obviously the case for the present experimental setup, and we define the anisotropy of the scattered γ rays as

$$A = \frac{\mu N_\perp - N_\parallel}{\mu N_\perp + N_\parallel}. \quad (2)$$

The normalization function $\mu(E_\gamma)$ can be determined from the ^{152}Eu source calibration and was found to be on the level of unity ±3% in the γ-ray energy range of interest,

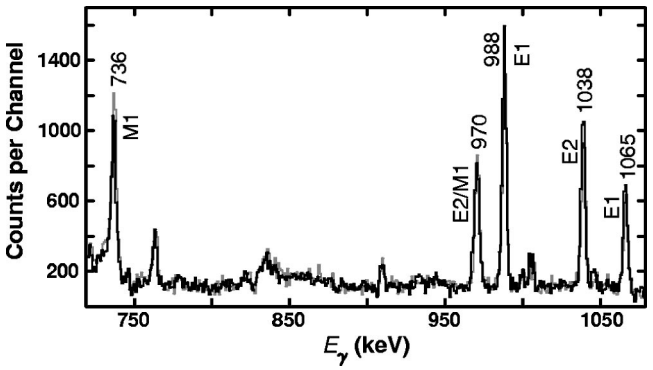

FIG. 1. Linear polarization spectra of in-plane (black) and out-of-plane (gray) scattered γ rays in coincidence with the 1038 and 1361 keV transitions in ^{61}Cu without any particle gating restriction. Transitions are labeled with their energies in keV and assigned multipolarity. See text for details.

i.e., 0.3 MeV $<E_\gamma<$ 2.0 MeV. The anisotropy A takes positive values for pure, stretched electrical radiation and negative values for pure, stretched magnetic radiation [12].

A fusion-evaporation reaction as the one in the present study populates excited states in some 20 to 30 different residual nuclei. The analysis with respect to angular correlations and especially linear polarization requires both statistics and unequivocally clean peaks in the γ-ray spectra. The former requires that the relative cross section of the residues has to be at least a few percent of the total fusion-evaporation cross section, whereas the latter is achieved by performing the analysis in $\gamma\gamma$ mode and eventually demanding a coincidence with an evaporated neutron. Thus four $\gamma\gamma$ matrices were created off line for the analysis: in-plane and out-of-plane Compton scattered γ-ray events in the CLOVER section vs γ rays detected anywhere in EUROBALL, both without any particle coincidence restriction and with coincidence of at least one detected neutron.

As many as possible clean coincidence spectra of the Compton scattered γ rays were created by gating on intense known peaks of several residual nuclei in these matrices, keeping the gating conditions for the in-plane and out-of-plane projections identical. To deduce the linear polarization of a given transition in a given isotope a certain subset of coincidence spectra was summed to increase the statistics. One example is illustrated in Fig. 1, which shows the summed spectra in coincidence with the 1038 and 1361 keV transitions in ^{61}Cu: While the anisotropies for the 988, 1038, and 1065 keV peaks are clear and positive, the anisotropy for the 970 keV line is close to zero and the one for the 736 keV line negative. In conjunction with the DCO ratios the multipolarities shown in Fig. 1 can be assigned easily (cf. Table I).

Figure 2 shows the clean separation of different types of

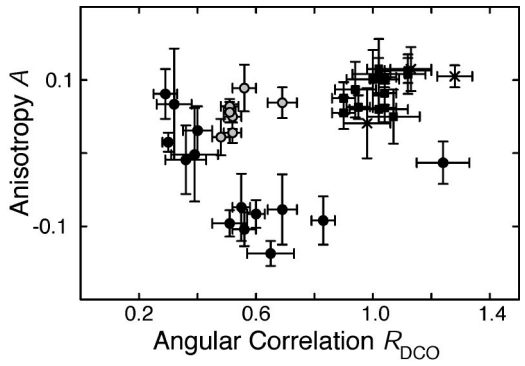

FIG. 2. Two-dimensional plot of the anisotropy A vs the angular correlation ratio R_{DCO}. Filled squares denote known and deduced $E2$ transitions, filled circles stretched $M1$ or mixed $E2/M1$ transitions, crosses parity-conserving $\Delta I=0$ transitions, and open circles stretched $E1$ transitions.

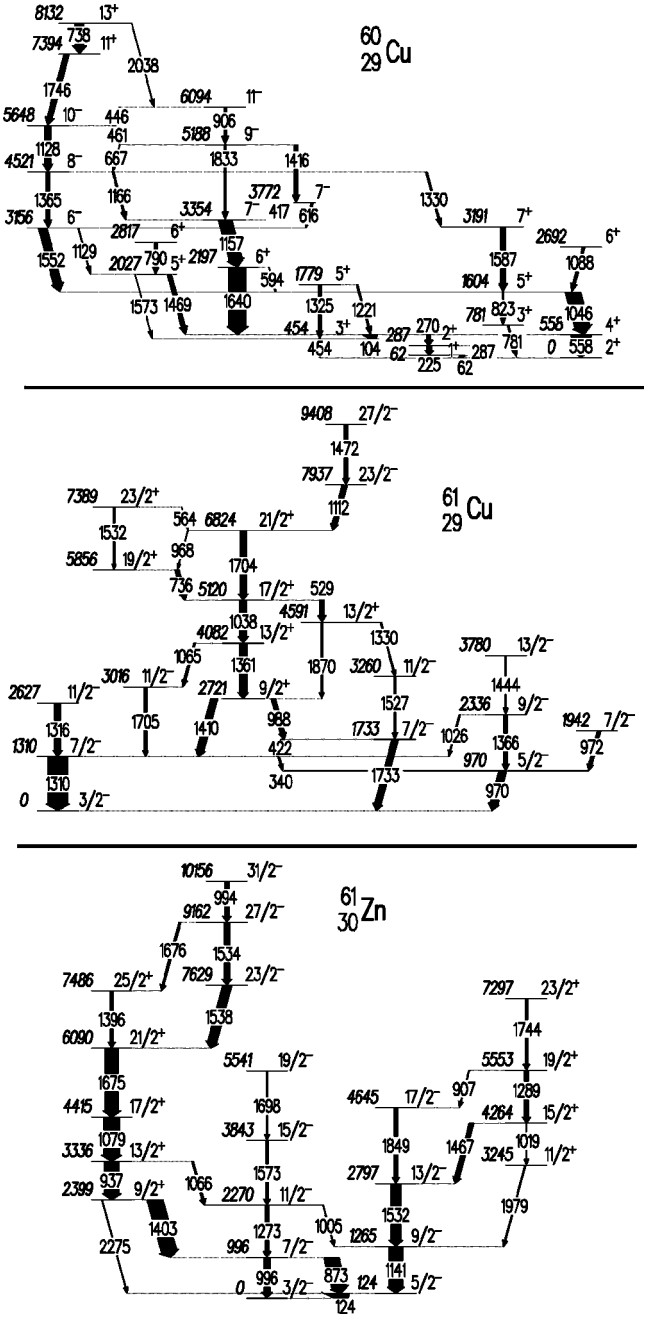

FIG. 3. Parts of the level schemes of ^{60}Cu, ^{61}Cu, and ^{61}Zn relevant for the present work. Energy labels are in keV and the thickness of the arrows reflects the relative intensities of the transitions.

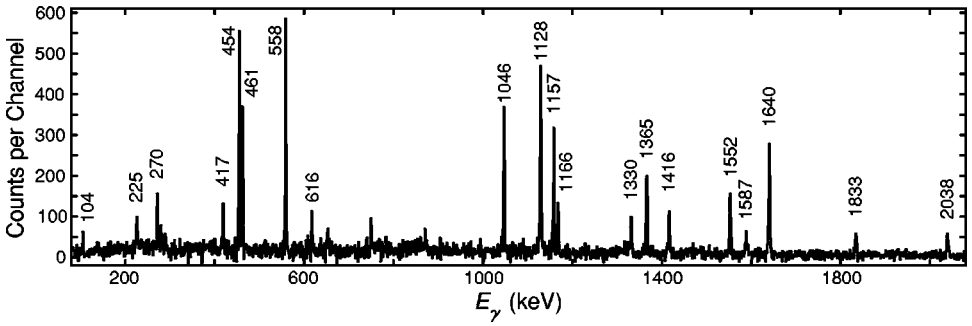

FIG. 4. Spectrum in coincidence with the 446 keV $11^- \rightarrow 10^-$ transition in ^{60}Cu. It is gated by three protons and one neutron detected in ISIS and the Neutron Wall, respectively. Peaks associated with ^{60}Cu are labeled with their energies in keV.

multipole radiation in a two-dimensional plot of anisotropy vs angular correlation as defined in Eqs. (1) and (2). There is only one ambiguity between stretched electric quadrupole radiation and $\Delta I=0$ $E2/M1$ radiation, which have both similar DCO ratios and anisotropies. However, such ambiguitites can be accounted for by means of yrast arguments—in high-spin studies the stretched transitions are usually much more intense than the non-stretched transitions—and information from parallel branches, which provide additional information on the relevant states.

Table I provides a short summary of the present study. A more comprehensive table can be found in Ref. [14]. The uncertainties in Table I are derived from standard error propagation formulas and include the uncertainties in the peak areas and of the efficiency corrections (DCO ratios) or the normalization function (anisotropies), respectively. Note that by calculating a difference in the numerator of Eq. (1), large (relative) uncertainties may occur for the anisotropy results.

Besides a number of reference transitions in mainly ^{61}Cu [15,2], Table I comprises the ~25 unambiguous parity-changing $E1$ transitions identified in ^{61}Zn, $^{60-61}$Cu, $^{57-60}$Ni, and ^{57}Co [2,15–21] as well as a large fraction of until now ambiguous or unknown transitions in ^{61}Zn [15,2] and ^{60}Cu [16,17]. For completeness, the relevant parts of the excitation schemes of ^{61}Zn and $^{60-61}$Cu are included in Fig. 3. They comprise about half the information from the present experiment and are subject to further detailed nuclear structure studies. Figure 4 presents an example of the quality of the full $\gamma\gamma$ data by means of a spectrum in coincidence with the new 446 keV $11^- \rightarrow 10^-$ transition in ^{60}Cu.

While the level schemes of the two copper isotopes are by and large in agreement with the most recent high-spin investigations [2,17], the decay scheme of ^{61}Zn is by far more comprehensive and complete compared to previous investigations. It comprises what one may interpret as signature partner bands for both negative and positive parity up to the maximally aligned seniority five states at $I=19/2^-$ and $25/2^+$. Furthermore, the excitation of one or two particles from the fp shell into the $1g_{9/2}$ orbital are clearly marked by the 1403 keV $9/2^+ \rightarrow 7/2^-$ and 1538 keV $23/2^- \rightarrow 21/2^+$ transitions, respectively.

In summary, reliable experimental information concerning parity-changing $E1$ transitions has been presented, which is considered an important contribution to the determination of a shell-model configuration space including both the fp shell and the $1g_{9/2}$ orbital. The position of $9/2^+$ states, presumably of single-particle character, has been supported or marked in the odd-A isotopes ^{57,59}Ni, ^{61}Cu, and ^{61}Zn.

The authors thank S. Kasemann and R. Darlington for the target preparation and the operating crew of the Legnaro Tandem for the excellent support. This research was supported in part by the Swedish Research Council and the European Commission TMR/LSF Contract No. ERBFMGECT980110.

[1] D. Rudolph, C. Baktash, M. J. Brinkman, M. Devlin, H.-Q. Jin, D. R. LaFosse, L. L. Riedinger, D. G. Sarantites, and C.-H. Yu, Eur. Phys. J. A **4**, 115 (1999).
[2] S. M. Vincent *et al.*, Phys. Rev. C **60**, 064308 (1999).
[3] S. M. Vincent *et al.*, Phys. Lett. B **437**, 264 (1998).
[4] D. Rudolph *et al.*, Phys. Rev. C **69**, 034309 (2004).
[5] F. Nowacki (private communication).
[6] *EUROBALL III, A European γ-ray facility*, edited by J. Gerl and R. M. Lieder (GSI, Darmstadt, Germany, 1992).
[7] P. M. Jones *et al.*, Nucl. Instrum. Methods Phys. Res. A **357**, 458 (1995).
[8] J. Eberth, H. G. Thomas, P. von Brentano, R. M. Lieder, H. M. Jäger, H. Kämmerling, M. Berst, D. Gutknecht, and R. Henck, Nucl. Instrum. Methods Phys. Res. A **369**, 135 (1996).
[9] Ö. Skeppstedt *et al.*, Nucl. Instrum. Methods Phys. Res. A **421**, 531 (1999).
[10] E. Farnea *et al.*, Nucl. Instrum. Methods Phys. Res. A **400**, 87 (1997).
[11] K. S. Krane, R. M. Steffen, and R. M. Wheeler, At. Data Nucl. Data Tables **11**, 351 (1973).
[12] P. J. Twin, in *The Electromagnetic Interaction in Nuclear Spectroscopy*, edited by W. D. Hamilton (North-Holland, Amsterdam, 1975), Chap. 15.
[13] A. von der Werth *et al.*, Nucl. Instrum. Methods Phys. Res. A **357**, 458 (1995).
[14] O. Izotova, Master thesis, Lund University, 2003, http://wwwnsg.nuclear.lu.se/projects.asp
[15] M. R. Bhat, Nucl. Data Sheets **88**, 417 (1999).
[16] M. M. King, Nucl. Data Sheets **69**, 1 (1993).
[17] Tsan Ung Chan *et al.*, Phys. Rev. C **26**, 424 (1982).
[18] S. Juutinen *et al.*, Nucl. Phys. **A504**, 205 (1989).
[19] M. R. Bhat, Nucl. Data Sheets **80**, 789 (1997).
[20] D. Rudolph *et al.*, Eur. Phys. J. A **6**, 377 (1999); Phys. Scr. **T88**, 21 (2000).
[21] O. L. Caballero, F. Cristancho, D. Rudolph, C. Baktash, M. Devlin, L. L. Riedinger, D. G. Sarantites, and C.-H Yu, Phys. Rev. C **67**, 024305 (2003).